

Дослідження присвячено підвищенню енергетичної ефективності вільновихрового насоса типу «Туро» шляхом удосконалення його робочого колеса. Це дозволяє мінімізувати загальну вартість життєвого циклу насосної установки у результаті зниження витрат на електроенергію.

Застосування фізичної моделі потоку реальної рідини у вільновихровому насосі дозволило розробити математичну модель розподілу енергії у його проточній частині. У запропонованій математичній моделі кількісно встановлено співвідношення складових потоків. До них віднесено тороподібний вихор, потік, що надходить із міжлопатевих каналів робочого колеса безпосередньо до відводу, і потік, що не контактує з лопатями (потік протікання). У результаті встановлено, що максимально можливий ККД робочого процесу вільновихрового насоса без урахування гідравлічних втрат складає $\eta_{pm}=0,67$.

Розроблено методіку конструювання робочого колеса з криволінійним профілем лопаті. Методіка базується на запропонованій математичній моделі розподілу енергії у проточній частині вільновихрового насоса. Кут установки лопаті на вході β_1 і на розрахунковому радіусі βr робочого колеса запропоновано виконувати відповідно до витрати рідини у міжлопатевих каналах робочого колеса. Радіус $r < r_2$ обирається таким, для якого спостерігається радіальний рух рідини у міжлопатевих каналах робочого колеса.

Виконання чисельного дослідження дало можливість оцінити структуру потоку у проточній частині вільновихрового насоса. Використання запропонованого робочого колеса дозволило мінімізувати втрати на вході та у його міжлопатевих каналах у результаті узгодження потоку рідини і геометрії скелету лопаті. Збільшення частки лопатевого і зменшення частки вихрового робочого процесу дозволило підвищити ККД вільновихрового насоса.

Запропонована геометрія робочого колеса дозволяє підвищити ККД існуючих вільновихрових насосів на 4–5 %

Ключові слова: вільновихровий насос, робоче колесо, проточна частина, ККД, інвестиційні витрати

A METHOD OF DESIGNING OF TORQUE-FLOW PUMP IMPELLER WITH CURVILINEAR BLADE PROFILE

V. Kondus
Assistant*

E-mail: vladislav.kondus@meta.ua

P. Kalinichenko

PhD, Associate Professor**

E-mail: KalinichenkoPavel57@gmail.com

O. Gusak

PhD, Associate Professor*

E-mail: gusak@pgm.sumdu.edu.ua

*Department of Applied Hydro- and Aeromechanics***

Department of general mechanics and dynamics of machines*

***Sumy State University

Rymkoho-Korsakova str., 2,
Sumy, Ukraine, 40007

1. Introduction

For transportation of untreated industrial and domestic waste, semi-finished products as viscous liquids, liquids with solid particles and fibrous inclusions, and various suspensions, torque-flow pumps are applied (Fig. 1).

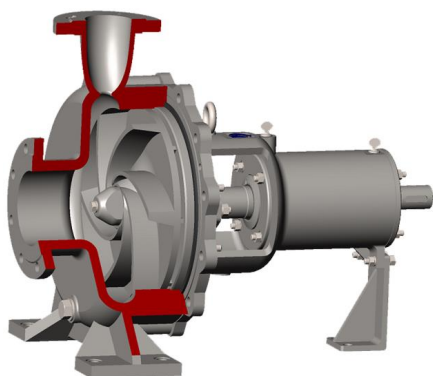


Fig. 1. The construction of a torque-flow pump

The design feature of torque-flow pumps is the presence of a free chamber in front of the impeller. The placement of the impeller in the pump casing cylindrical niche and the free passage of the fluid flow through the free chamber allows the pumping of mixtures with a high concentration of solid impurities without changing the operating parameters of the pump.

In centrifugal pumps, the entire fluid flow passes through the impeller intervane channels. In a torque-flow pump, the fluid partially passes through them. The other part is routed through a free chamber without interacting with the blades.

The main disadvantage of torque-flow pumps is the low value of their energy efficiency, which does not exceed 58–60 %. As a result, the costs of electricity in the life cycle cost of a pump installation using a torque-flow pump is greater than using a centrifugal pump. However, for the transport of liquids containing the inclusions, the life cycle cost of a pump installation using a torque-flow pump is less, resulting in significantly lower maintenance costs [1].

For today, most torque-flow pumps are equipped with impellers with straight radial (Fig. 2, a), or made with some

outlet angle β_2 (Fig. 2, *b*), blades. Replacing the impeller with a curvilinear profile of the blade (Fig. 2, *c*) is promising in view of increasing the energy efficiency of existing torque-flow pumps. At the same time, the investment costs will be minimal.

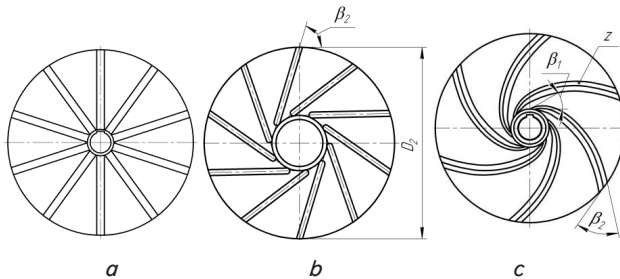


Fig. 2. Design of the torque-flow pump impeller: *a* – with radial blades; *b* – with straight blades with outlet angle $\beta_2=80^\circ$; *c* – with a curvilinear blade profile

The topicality of the study is to develop a method of designing a torque-flow pump impeller with a curvilinear profile of a blade. This will significantly increase the energy efficiency of torque-flow pumps.

2. Literature review and problem statement

In the paper [2], the influence of the impeller design elements on the operating parameters of the torque-flow pump was considered. The study determined the effect of changing the impeller design elements (number of blades z , blade inlet β_1 and outlet β_2 angles of the impeller) on the nominal pump operating parameters. However, the effect of the simultaneous change of the blade inlet β_1 and outlet β_2 angles of the impeller in this paper was not investigated.

The study [3] made a qualitative assessment of the effect of changing the impeller parameters on the nominal operating parameters of torque-flow pumps. The research was conducted with pumps with different specific speeds n_s . However, the optimal parameters at which maximum pump energy efficiency was reached were not defined, and the method of their designing was not offered.

In the paper [4], a complex study of the influence of impeller geometric parameters on the torque-flow pump characteristics has been carried out. The author replaced the impeller with straight blades with the impeller with the curvilinear blade profile. The increasing of the torque-flow pump energy efficiency by 4–5%, as a result of the impeller replacement was proved experimentally. The disadvantage of the study is the lack of recommendations for determining the blade inlet β_1 and outlet β_2 angles of the impeller for pumps with different specific speeds n_s .

Using winglets on the blades of a torque-flow pump impeller allowed increasing the pump head [5]. However, in order to provide high parameters, the increasing of the gap between the impeller and the pump casing by at least 10 mm is necessary [6]. The disadvantage of the paper is overall pump dimensions increasing. Thus, a similar result can be achieved by simply increasing the pump impeller diameter.

The increasing of torque-flow pumps energy efficiency is achieved by influencing the pump casing construction [7]. However, such a way of increasing the pumps energy efficien-

cy leads to a significant increasing of investment costs in the existing pumps modernization.

The study [8] showed a qualitative picture of fluid flow in a torque-flow pump. The paper was done using the method of high-speed filming of motion of different-length strings. However, this method did not allow quantifying the fluid flow in the pump flowing part. Thus, the obtained results do not allow formulating recommendations concerning the method of designing the pump impeller.

In the paper [9], the approximate theoretical value of the energy efficiency of the vortex operating process of the torque-flow pump was determined. The research was based on the laws of conservation of the angular momentum and energy. However, the described mathematical model did not allow quantifying the energy distribution in the pump flowing part.

Application of modern modeling methods allows more accurate estimation of qualitative and quantitative characteristics of the fluid flow in the flowing part of rotary hydromachines. The test tasks of studying the operating process of a torque-flow pump based on the numerical investigation method using the Ansys CFX software product were discussed in the following papers. The study of cavitation processes in the pumps flowing part was made in a non-stationary formulation [10]. In the paper [11], in the stationary formulation the integral characteristics of the torque-flow pump were determined. The obtained results differed from the experimental data by no more than 5% in the operating range. This does not exceed the permissible error of experimental research methods. As a result, it has been proven that this software product can be used to improve the torque-flow pumps design.

The conducted literature review allows drawing the following conclusion. For today there is no reliable literature information on determining the optimum values of the blade inlet β_1 and outlet β_2 angles of the torque-flow pumps impeller with different values of the specific speed n_s . Studies of this issue are separated and cannot be described as systemic. The peculiarities of the operating process of this type pumps include the presence of a flow portion (flowing stream) that does not interact with the impeller blades, as well as the presence of a toroidal vortex in their flowing part. The lack of a reliable mathematical model of energy distribution in the torque-flow pump flowing part does not allow estimating the blade and vortex parts of its operating process, as well as determining the maximum possible energy efficiency of the vortex operating process. There is no method of designing the torque-flow pump impeller with a curvilinear blade profile, which complicates the process of its design.

3. The aim and objectives of the study

The aim of the present study is to develop a method of improving a torque-flow pump impeller with a curvilinear blade profile for increasing its energy efficiency.

To achieve the aim, the following tasks are necessary to accomplish:

- to develop a mathematical model of energy distribution in the torque-flow pump flowing part;
- to develop a method of designing a pump impeller blade;
- to determine the effect of the blade construction on the fluid flow in the pump flowing part using the numerical investigation method.

4. Method of numerical investigation of fluid flow in a torque-flow pump

To achieve the stated aim, the research was carried out using the method of numerical solution of the problem. The calculation model was created in the Ansys CFX environment.

As an operating environment, water at a temperature of 25 °C was used. The operating mode was turbulent. For closing the Reynolds equations, a standard $k-\epsilon$ turbulence model was used.

The calculated region consists of two elements: stator – the pump casing flowing part, and rotor – the impeller. For each of the elements of the calculated region, an unstructured calculation grid was constructed. The total number of elements of the calculated grid is 1 million 500 thousand cells. The flow modeling was carried out in a stationary setting.

The mass flow rate through the pump flowing part was set as the boundary condition at the inlet of the calculated region. Pressure equal to 1 MPa acted in the role of the boundary condition at the outlet from the calculated region.

Due to the reverse currents, at the outlet of the calculated region of the stator element, “opening” was specified as the boundary condition.

The rotational frequency for all experiments in the series has a value of $n=1500$ rpm.

In order to achieve the convergence of the results, a numerical investigation was conducted with the task of interaction interface between the calculated regions “Frozen rotor”. In order to refine the data, the obtained results were used as initial values during a numerical investigation with the task of the interaction interface between the calculated areas “Stage”.

5. Results of investigation of fluid flow in the torque-flow pump

5.1. Mathematical model of energy distribution in the torque-flow pump flowing part

The model described in the study [12] is chosen as a base of the physical model of the torque-flow pump fluid flow (Fig. 3).

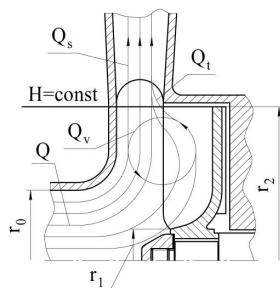


Fig. 3. Physical model of fluid flow motion in the torque-flow pump flowing part: Q_t – flow coming from the impeller directly to the pump outlet (through-flow); Q_s – flow that does not interact with the impeller blades (flowing stream); Q_v – toroidal vortex

At the inlet of the torque-flow pump, a part of the fluid enters the impeller. Under the influence of centrifugal forces, it throws to the periphery. Due to the presence of the stator wall of a pump casing, the fluid changes the direction perpendicular to the disk of the impeller. The flow, which enters the

free chamber from the impeller, is divided into two parts. The first part, through-flow (Q_t), comes from the impeller directly into the discharge nozzle of the pump. The other part forms a toroidal vortex (Q_v) in a free chamber of the pump.

The flow that does not come into contact with the blades (flowing stream, Q_s) enters the pump outlet without interacting with the impeller blades. The energy transfer occurs due to the exchange of the angular momentum with a toroidal vortex in the free chamber of the pump.

Thus, in a torque-flow pump there is a complex process of energy transfer, consisting of two stages:

- transfer of energy to the through-flow (blade operating process);
- transfer of energy from the toroidal vortex to the flowing stream (vortex operating process).

A toroidal vortex in the vortex operating process acts as a so-called “liquid blade”. In conjunction with it, the flowing stream acquires an increase of energy.

In order to construct a mathematical model of energy distribution, three conditions were used, which were the necessary conditions for the steady fluid flow in the torque-flow pump flowing part.

Firstly, this is the equality of the specific energy at the impeller outlet (Fig. 3). In this case, the head is the specific energy of the unit of weight of the liquid:

$$H_i = H_s, \tag{1}$$

where H_i – the head created by the impeller; H_s – the head of the flowing stream at the outlet of the impeller.

Secondly, it is the equality of the hydraulic power of the through-flow and the hydraulic power of the flowing stream:

$$N_{ht} = N_{hs}, \tag{2}$$

where N_{ht} – hydraulic power of the through-flow; N_{hs} – hydraulic power of the flowing stream.

Thirdly, this is the equality of the energy of the flowing stream and the through-flow at the impeller outlet:

$$\rho g Q_s H_s = \rho g Q_t H_t, \tag{3}$$

where H_t – the head of the through-flow.

Based on (3), the flow rate of the through-flow and the flow rate of the flowing stream are equal:

$$Q_s = Q_t. \tag{4}$$

In the process of transferring energy from a toroidal vortex to a flowing stream, there is a leveling of energy. Thus, only half of the hydraulic power is transmitted:

$$\frac{1}{2} \rho g Q_v H_t = \rho g Q_s H_s. \tag{5}$$

Proceeding from (5), we established the ratio of the fluid amount which forms the toroidal vortex and the flowing stream:

$$\frac{1}{2} Q_v = Q_s. \tag{6}$$

Taking into account (4) and (6), the ratio between the toroidal vortex and the through-flow was deduced:

$$\frac{1}{2}Q_v = Q_t \tag{7}$$

The maximum possible energy efficiency of the torque-flow pump operating process without taking into account the hydraulic losses is the ratio of useful hydraulic power to the hydraulic power, which is created by the impeller:

$$\eta_{op} = \frac{N_h}{N_{hi}} = \frac{\frac{2}{3}N_{hi}}{N_{hi}} = 0.67, \tag{8}$$

where N_{hi} – hydraulic power, which is created by the impeller.

Taking into account (8), the energy efficiency of the torque-flow pump is determined by the dependence:

$$\eta = \eta_{op} \eta_h \eta_m, \tag{9}$$

where η_h – hydraulic energy efficiency of the torque-flow pump; η_m – mechanical energy efficiency of the torque-flow pump.

The proposed mathematical model represents the dependence of the torque-flow pump energy efficiency of its blade and vortex parts. The part of the blade operating process was represented as the hydraulic power of the through-flow. The part of the vortex operating process was given in the form of hydraulic power of the flowing stream.

It was found that the maximum possible energy efficiency of the torque-flow pump operating process is 0.67.

5. 2. Method of designing torque-flow pump impeller blade

In order to determine the blade inlet β_1 and outlet β_2 angles of the torque-flow pump impeller, the fluid flow in its intervane channels should be considered. At the same time, the fluid velocity components are decomposed into components (Fig. 4).

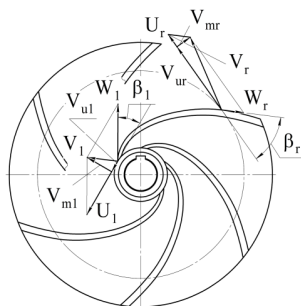


Fig. 4. Triangles of velocities in the torque-flow pump impeller

The direction of fluid flow near the impeller radius r_2 is changed due to the presence of a cylindrical niche of the pump casing. Therefore, it is advisable to construct triangles of velocities at the inlet of the impeller, and for some radius r , which is slightly less than r_2 . The radius r is characterized by the direction of the fluid flow from the center to the periphery of the impeller.

Torque-flow pumps are projected without fluid rotating at the inlet of the impeller. It means that $V_{u1}=0$. In this way, the maximum pump head at high energy efficiency is ensured.

The blade inlet angle is determined by the dependence:

$$\beta_1 = \arctg \frac{Q_i}{2\pi r_1^2 b_1 \omega}, \tag{10}$$

where $Q_i=Q_t+Q_v$ – flow rate through intervane channels of the impeller; r_1 – the impeller inlet radius; b_1 – the impeller inlet width; ω – angular velocity of the impeller.

The blade outlet angle is determined by the dependence:

$$\beta_r = \arctg \frac{Q_i}{2\pi r b_r (\omega r - V_{ur})}, \tag{11}$$

where b_r – the impeller width at the radius r ; ω – angular velocity of the impeller; V_{ur} – circumferential component of absolute velocity at the radius r .

The blade skeleton is connected with the achievement of a smooth transition from the blade inlet angle value β_1 to the blade angle value at a certain radius β_r .

6. Results of the investigation of the torque-flow pump operating process

In order to research the torque-flow pump operating process, the analysis of the fluid flow structure in the flowing part, in accordance with the cross sections, was performed (Fig. 5).

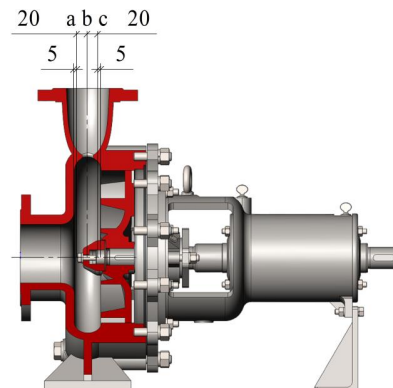


Fig. 5. Location of cross sections in the flow structure analysis in the pump

The distribution of the axial component of the absolute velocity V_z (Fig. 6) allows quantifying the fluid flow through the pump impeller.

The nature of the change in the radial component of the absolute velocity V_R (Fig. 7) proves the presence of a toroidal motion in the torque-flow pump operating process.

The fluid flow structure according to calculating diameters was considered for the refinement of the obtained data (Fig. 8).

The distribution of the axial component of the absolute velocity V_z (Fig. 9) in the torque-flow pump free chamber at the diameters: d_{hub} (Fig. 9, a): $d=158$ mm (Fig. 9, b), $d=242$ mm (Fig. 9, c) and D_2 (Fig. 9, d).

The distribution of the static pressure p (Fig. 10) in the torque-flow pump free chamber was defined at the diameters: d_{hub} (Fig. 10, a), $d=158$ mm (Fig. 10, b), $d=242$ mm (Fig. 10, c) and D_2 (Fig. 10, d). The horizontal axis indicates the ratio of the distance of the calculated point from the wall of the pump casing to the width of the free chamber $\bar{B} = \frac{b}{B}$.

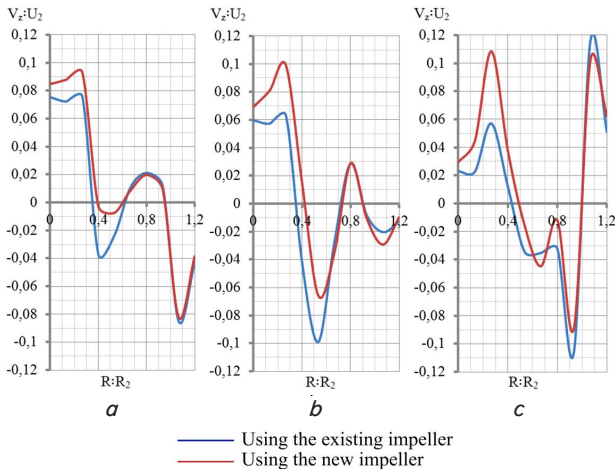


Fig. 6. Distribution of the axial component of the absolute velocity V_z in the torque-flow pump free chamber: *a* – near the wall of the pump casing; *b* – in the middle of a free chamber; *c* – near the impeller

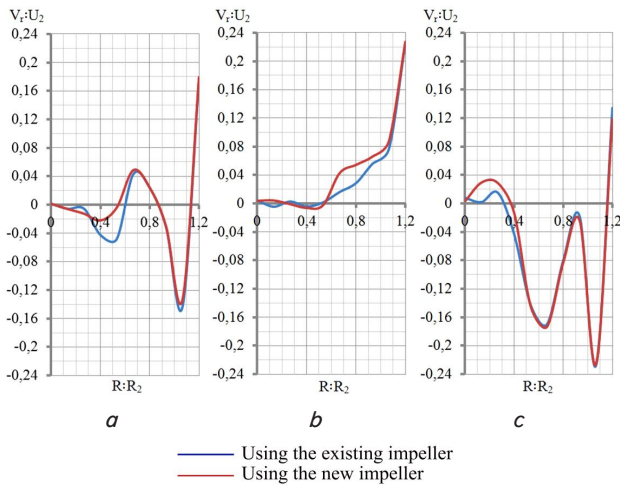


Fig. 7. Distribution of the radial component of the absolute velocity V_r in the torque-flow pump free chamber: *a* – near the wall of the pump casing; *b* – in the middle of a free chamber; *c* – near the impeller

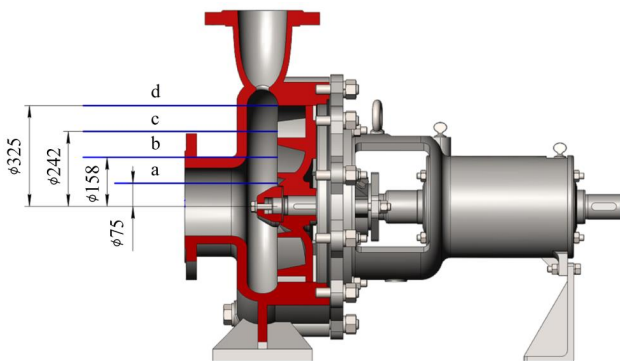


Fig. 8. Location of calculating diameters in the course of analyzing the fluid flow structure in the pump

An even distribution of static pressure in a torque-flow pump free chamber near the outer diameter D_2 of the impeller (Fig. 10, *d*) has been experimentally proved.

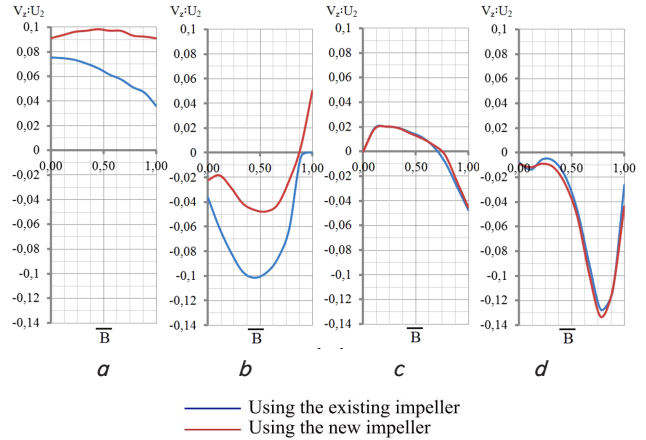


Fig. 9. Distribution of the axial component of the absolute velocity V_z in the torque-flow pump free chamber at the diameters: *a* – d_{hub} ; *b* – $d=158$ mm; *c* – $d=242$ mm; *d* – D_2

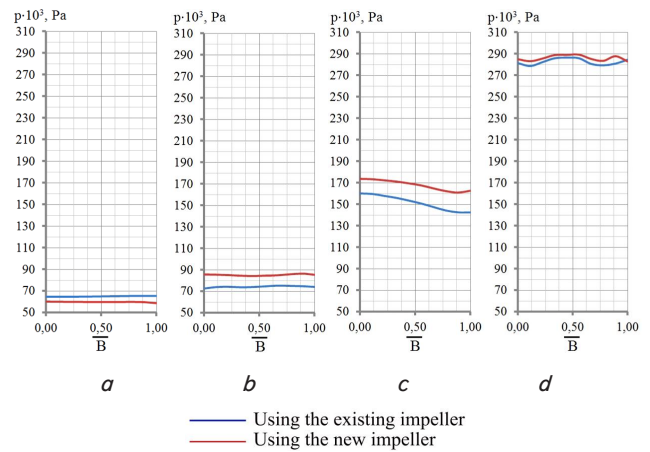


Fig. 10. Distribution of the static pressure p in the torque-flow pump free chamber at the diameters: *a* – d_{hub} ; *b* – $d=158$ mm; *c* – $d=242$ mm; *d* – D_2

7. Discussion of the results of investigation of torque-flow pump operating process

The graphs of the distribution of the axial component of the absolute velocity V_z (Fig. 6) prove that the larger volume of fluid enters into the new impeller than into the existing one. So in the range of calculating radius values $R/R_2 = 0-0.5$ the value of this velocity component is higher using the new impeller. However, at the impeller outlet, the fluid flow rate is equal for both ones.

The calculated graphs prove that the value of the axial component of the absolute velocity V_z at the inlet (Fig. 9, *a*) and at the diameter $d=158$ mm (Fig. 9, *b*) is higher when the new impeller is used. In this case, its distribution in the torque-flow pump free chamber at the diameter $d=242$ mm (Fig. 9, *c*) and near the impeller outer diameter D_2 (Fig. 9, *d*) is identical.

The obtained result is caused by the coordination of the fluid flow angle and the blade inlet angle β_1 , as well as less losses in intervane channels of the impeller. As a result, the flow resistance at the impeller inlet is smaller using a new impeller. Thus, the fluid freely passes through the impeller intervane channels and heads to its periphery.

One can conclude that when replacing an existing impeller with a new one, the fluid volume in the vortex operating process Q_v decreases. In this case, the through-flow Q_t increases. As a result of increasing the blade and decreasing the vortex part, the energy efficiency of the torque-flow pump operating process increases.

This phenomenon is also confirmed in the study of the radial component of absolute velocity V_r in the torque-flow pump free chamber (Fig. 7). It is higher inside the pump free chamber at the calculating radius in the range $R/R_2 = 0.5-1.1$ using a new impeller than using an existing one. This is due to decreasing the fluid amount in the vortex operating process. The fluid motion in a toroidal vortex occurs in the direction from the outlet to the inlet of the impeller, that is, in the opposite direction of the flowing stream. Thus, with decreasing the vortex operating process part, increasing the radial component of the absolute velocity V_r is observed.

The unevenness of the static pressure distribution at the diameter $d=242$ mm (Fig. 10, c) is caused by decreasing the absolute velocity in the direction from the blades edge to the wall of the pump casing. As a result, static pressure increases.

The proposed mathematical model of energy distribution in the torque-flow pump flowing part allows quantifying the blade and vortex parts of its operating process. The obtained results allowed developing the method of designing the torque-flow pump impeller blade in view of volumes of the through-flow Q_t , as well as toroidal vortex Q_v .

The advantage of the proposed method is the ability to design a torque-flow pump impeller with a wide range of specific speed n_s . This is an advantage of the proposed method in relation to the experimental results obtained earlier.

Replacing the existing impeller with straight blades with the new one with a curvilinear blade profile has allowed increasing the torque-flow pump energy efficiency by 4–5 % [4].

Theoretically calculated impeller blade inlet angle β_1 of the torque-flow pump SVN 80/32 is estimated at 33°. This corresponds to the value of this angle at which the maximum value of the pump energy efficiency is experimentally obtained [4]. Theoretically calculated impeller blade angle β , at

the radius $r=0.8r_2$ of the torque-flow pump SVN 80/32 with $n_s=60$ is 44°. The difference from the experimental value of this angle is less than 3° [4].

The complexity of further research is related to the complex structure of the fluid flow in the torque-flow pump flowing part.

8. Conclusions

1. The mathematical model of energy distribution in the torque-flow pump flowing part was developed. As a result, the quantitative distribution of the flowing stream Q_s , the toroidal vortex Q_v , as well as the through-flow Q_t , was determined. The maximum possible efficiency of the torque-flow pump operating process is $\eta_{op}=0.67$.

2. The method of designing an impeller with a curvilinear blade profile has been developed. It is based on a mathematical model of energy distribution in the pump flowing part. The method allows reconciling the fluid flow with the geometry of the blade skeleton. The proposed method can be used in the design of the impeller blade in the whole range of values of the specific speed n_s , in which torque-flow pumps are used. So, for a pump SVN 80/32 with specific speed $n_s=60$ theoretically calculated the impeller blade inlet angle is $\beta_1=33^\circ$, for which the maximum energy efficiency of the pump has been experimentally achieved. Theoretically calculated impeller blade angle β , at the impeller radius $r=0.8r_2$ of the torque-flow pump SVN 80/32 is 44°. This corresponds to the experimental results.

3. The proposed impeller blade design allows reducing the vortex part and increasing the blade part of torque-flow pump operating process. This occurs by coordination of the fluid flow angle and the impeller blade inlet angle β_1 , as well as reducing losses in the impeller intervan channels. As a result of reducing the resistance at the impeller inlet, the fluid freely enters impeller intervan channels and heads to the periphery. As a result, the torque-flow pump energy efficiency using a new impeller is 4–5 % higher than using the existing impeller.

References

1. Kotenko A., Herman V., Kotenko A. Rationalisation of Ukrainian industrial enterprises in a context of using torque flow pumps on the basis of valuation of the life cycle of pumping equipment // *Nauka i Studia*. 2014. Issue 16 (126). P. 83–91.
2. Optimization design and test of vortex pump based on CFD orthogonal test / Gao X., Shi W., Zhang D. et. al. // *Nongye Jixie Xuebao/Transactions of the Chinese Society for Agricultural Machinery*. 2014. Vol. 45, Issue 5. P. 101–106.
3. Design Parameters of Vortex Pumps: A Meta-Analysis of Experimental Studies / Gerlach A., Thamsen P., Wulff S., Jacobsen C. // *Energies*. 2017. Vol. 10, Issue 1. P. 58. doi: 10.3390/en10010058
4. Kondus V., Kotenko A. Investigation of the impact of the geometric dimensions of the impeller on the torque flow pump characteristics // *Eastern-European Journal of Enterprise Technologies*. 2017. Vol. 4, Issue 1 (88). P. 25–31. doi: 10.15587/1729-4061.2017.107112
5. Gerlach A., Thamsen P., Lykholt-Ustrup F. Experimental Investigation on the Performance of a Vortex Pump using Winglets // *ISROMAC 2016. International Symposium on Transport Phenomena and Dynamics of Rotating Machinery*. 2016. P. 10–15.
6. Chervinka M. Computational Study of Sludge Pump Design with Vortex Impeller // *18th International Conference ENGINEERING MECHANICS 2012*. 2012. P. 191–201.
7. Krishtop I. Creating the flowing part of the high energy-efficiency torque flow pump // *Eastern-European Journal of Enterprise Technologies*. 2015. Vol. 2, Issue 7 (74). P. 31–37. doi: 10.15587/1729-4061.2015.39934
8. Study on clogging mechanism of fibrous materials in a pump by experimental and computational approaches / Kudo H., Kawahara T., Kanai H., Miyagawa K., Saito S., Isono M. et. al. // *IOP Conference Series: Earth and Environmental Science*. 2014. Vol. 22, Issue 1. P. 012011. doi: 10.1088/1755-1315/22/1/012011
9. Evtushenko A. A. Osnovy teorii rabocheho protsessa vzhrevyih gidromashin // *Tehnologicheskie sistemy*. 2002. Issue 2 (13). P. 110–113.

10. Kotenko A., Nikolaenko L., Lugova S. The computational model of the emergence and development of cavitation in torque flow pump // 4th International Meeting on Cavitation and Dynamic Problems in Hydraulic Machinery and Systems. 2011. P. 87–94.
11. Numerical Approach for Simulation of Fluid Flow in Torque Flow Pumps / Krishtop I., German V., Gusak A., Lugova S., Kochevsky A. // Applied Mechanics and Materials. 2014. Vol. 630. P. 43–51. doi: 10.4028/www.scientific.net/amm.630.43
12. Grabow G. Einfluss der Beschauelfung auf das Kennlinie Verhalten von Freistrompumpen // Pumpen und Verdichter. 1972. Issue 2. P. 18–21.

У даному дослідженні було розроблено нову суцільну конструкцію теплових труб для підвищення теплових характеристик. Вивчення кипіння у суцільній тепловій трубі досліджується для детальної інформації про зародження бульбашок. Експеримент проводився в суцільних теплових трубах з варіацією випарника (d) до співвідношення діаметра конденсатора (D). Значення d/D змінюються в $1/1$; $1/2$; $1/3$ і $1/4$. Теплове навантаження генерується на секції випарника з використанням DC-Power нагрівача на 30, 40 та 50 Вт. Технологія візуалізації була розроблена за допомогою прозорої скляної трубки, а знімки киплячих бульбашок були зроблені дзеркальною камерою. Нахил скляної труби становить 45° та інтегровано з модулем NI-9211 та c-DAQ 9271. Термомари K-типу встановлювалися на випарнику та конденсаторних секціях для вимірювання температури кипіння в суцільній тепловій трубі.

Виходячи з результатів, можна зазначити, що різні варіації співвідношення теплового навантаження та співвідношення діаметра (d/D) випарника та конденсатора впливають на розмір і форму киплячих бульбашок, а також температуру зародження на суцільній теплової трубі. Коефіцієнт теплопередачі має тенденцію до збільшення при тепловому навантаженні 50 Вт та співвідношенні діаметра $d/D=1/4$

Ключові слова: візуалізація кип'ятіння, утворення бульбашок, конічна труба теплопоглинання, коефіцієнт випаровування до діаметра конденсатора

1. Introduction

Heat pipe is a technology that uses porous media in the form of wick, which serves as a path for the return of liquid fluid from the condenser to the evaporator. The basic principle Heat pipe uses two-phase flow, latent heat and capillary channel for working fluid circulation between heating and cooling areas with wick media. The structure, design and construction of wick had a strong influence on heat pipe

performance and had a critical aspect in the manufacturing process.

The working system of heat pipe at a certain pressure, the liquid will evaporate, while the steam will also melt at a certain temperature, so that there will be pressure settings in the heat pipe which in turn will also regulate the working temperature and phase changes from liquid to vapor and vice versa. The capillary pressure in the wick will move fluid even against gravity due to the effect of capillarity.

UDC 62-67

DOI: 10.15587/1729-4061.2018.133973

VISUALIZATION OF BUBBLES FORMATION ON THE BOILING PROCESS IN TAPERING HEAT PIPE WITH VARIATION OF EVAPORATOR TO CONDENSER DIAMETER RATIO

Sarip

Doctoral Student

Department of Mechanical Engineering
Ronggolawe Technology High School
Jalan. Campus Ronggolawe Blok B/1,
Cepu, Indonesia, 58312
Central Java Indonesia.

E-mail: hidayatullohsarip566@gmail.com

Sudjito Soeparman

Professor, Researcher*

E-mail: sudjitospn@ub.ac.id

Lilis Yuliati

Doctor of Mechanical Engineering, Researcher*

E-mail: lilis_y@ub.ac.id

Moch. Agus Choiron

Doctor of Mechanical Engineering, Researcher*

E-mail: agus_choiron@ub.ac.id

*Department of Mechanical Engineering

University of Brawijaya Malang

Jalan. Mayjend Haryono, 167, Malang, Indonesia, 65145